



Human NPCs can degrade α -syn fibrils and transfer them preferentially in a cell contact-dependent manner possibly through TNT-like structures

Clara Grudina, Georgia Kouroupi, Takashi Nonaka, Masato Hasegawa,
Rebecca Matsas, Chiara Zurzolo

► To cite this version:

Clara Grudina, Georgia Kouroupi, Takashi Nonaka, Masato Hasegawa, Rebecca Matsas, et al.. Human NPCs can degrade α -syn fibrils and transfer them preferentially in a cell contact-dependent manner possibly through TNT-like structures. *Neurobiology of Disease*, 2019, 132, pp.104609. 10.1016/j.nbd.2019.104609 . pasteur-02941667

HAL Id: pasteur-02941667

<https://pasteur.hal.science/pasteur-02941667>

Submitted on 20 Jul 2022

HAL is a multi-disciplinary open access archive for the deposit and dissemination of scientific research documents, whether they are published or not. The documents may come from teaching and research institutions in France or abroad, or from public or private research centers.

L'archive ouverte pluridisciplinaire **HAL**, est destinée au dépôt et à la diffusion de documents scientifiques de niveau recherche, publiés ou non, émanant des établissements d'enseignement et de recherche français ou étrangers, des laboratoires publics ou privés.



Distributed under a Creative Commons Attribution - NonCommercial 4.0 International License

Human NPCs can degrade α -syn fibrils and transfer them preferentially in a cell contact-dependent manner possibly through TNT-like structures

Clara Grudina¹, Georgia Kouroupi², Takashi Nonaka³, Masato Hasegawa³, Rebecca Matsas² and Chiara Zurzolo^{1*}

¹ Unité de Trafic Membranaire et Pathogénèse, Institut Pasteur, 28 Rue du Dr. Roux Paris 75015, France.

² Laboratory of Cell and Molecular Neurobiology – Stem Cells, Department of Neurobiology, Hellenic Pasteur Institute, 127 Vassilissis Sofias Avenue, Athens 11521, Greece

³ Dementia Research Project, Tokyo Metropolitan Institute of Medical Science, 2-1-6 Kamikitazawa, Setagaya-ku, Tokyo 156-8585, Japan

*Corresponding author e-mail: chiara.zurzolo@pasteur.fr

Highlights

- α -syn fibrils are internalized by hNPCs and directed to lysosomes.
- α -syn fibrils are degraded over time by hNPCs.
- α -syn fibrils can propagate between hNPCs preferentially in a cell contact dependent manner possibly in TNT-like structures.

Abstract

Parkinson's disease (PD) is the second most common neurodegenerative disorder whereby loss of midbrain dopaminergic neurons results in motor dysfunction.

Transplantation of human induced pluripotent stem cells (iPSCs) into the brain of patients affected by PD is one of the therapeutic approaches that has gained interest to compensate for the degeneration of neurons and improve disease symptoms. However, only a part of transplanted cells can differentiate into mature neurons while the majority remains in undifferentiated state. Here we investigated whether human neuronal precursor cells (hNPCs) derived from iPSCs have an active role in α -synuclein (α -syn) pathology. Our findings demonstrate that α -syn fibrils are taken up by hNPCs and are preferentially localized in lysosomes where they can be degraded. However, α -syn fibrils are also transferred between hNPCs in a cell-to-cell contact dependent manner, and are found in tunneling nanotube (TNT)-like structures. Thus, NPCs can have a dual role in the progression of α -syn pathology, which should be considered in human transplants.

Keywords

Parkinson's disease; human neuronal precursors; alpha-synuclein; lysosomes; TNT-like structures

Abbreviations

PD, Parkinson's disease; α -syn, α -synuclein; iPSCs, induced pluripotent stem cells; hNPCs, human neuronal precursor cells; TNTs, tunneling nanotubes; TH, tyrosine hydroxylase.

1.Introduction

α -Synuclein (α -syn) is a presynaptic protein that plays a central role in the pathogenesis of a group of neurodegenerative diseases defined as

synucleinopathies, including Parkinson disease (PD). Intracellular deposits of aggregated α -syn within the neuron's soma and neurites, respectively known as Lewy bodies and Lewy neurites (Braak et al., 1999), are key features in these pathologies. Despite progress, the physiological functions of α -syn are still unclear. Several studies have shown that α -syn is involved in compartmentalization, storage, and recycling of neurotransmitters (Allen Reish and Standaert, 2015). A key feature for the pathological role of this protein is that it exists in different conformations, including monomeric and oligomeric states, that promote or impede its aggregation (Conway et al., 1998; Karpinar et al., 2009; Nuber et al., 2018). Furthermore different mutations of the protein, such as p.A53T cause autosomal dominant forms of PD (Tan et al., 2005) and can strongly promote and accelerate α -syn aggregation.

The cellular mechanisms underlying the initiation and propagation of α -syn pathology are still under investigation. Previous studies have shown that α -syn aggregates can spread in a prion-like manner from cell-to-cell in the brain *in vitro* as well as *in vivo* (Desplats et al., 2009; Freundt et al., 2012; Sacino et al., 2014; Peelaerts et al., 2015; Abounit et al., 2016; Brundin and Melki, 2017). Particularly, we have reported that mouse neuronal cells and primary neurons efficiently internalize fluorescent α -syn fibrils, direct them to lysosomal vesicles and transfer them to other neurons inside lysosomes in a contact-dependent manner through TNTs (Abounit et al., 2016). Moreover, we have shown that astrocytes can internalize α -syn fibrils and transfer them efficiently to astrocytes but not to neurons, indicating that the capacity to transfer fibrils can be cell-dependent. However differently from neurons, astrocytes are able to efficiently degrade fibrillar α -syn, suggesting an active role for these cells in clearing α -syn deposits (Loria et al., 2017).

Until now, no therapy is available to hold up or at least slow down the progress of neurodegeneration in the brain of PD patients. One approach that has gained considerable attention is the development of cell-based therapies to compensate dopaminergic neuronal loss and dopamine deprivation with new healthy neurons inducing major, long-lasting improvement. Although it is still unclear whether dopaminergic neuron degeneration is an initial feature of the disease or the unavoidable result of multiple dysfunctions throughout the brain, it represents a common pathological manifestation in PD and is responsible for many of the clinical symptoms, including motor dysfunction. Therefore several cellular sources have been considered for transplantation, including human induced pluripotent stem cells (iPSCs). However, a crucial aspect in this approach is that the transplanted cells must survive for a long time, differentiate to the appropriate neuronal phenotype and finally integrate into the host tissue. Recent studies have demonstrated that 6-54% of the transplanted cells survive and express tyrosine hydroxylase (TH) at 6–18 weeks in a rat model (Freed et al., 2001; Kriks et al., 2011) whilst only $33.3 \pm 24.4\%$ become TH positive at 6 months in a primate model (Kikuchi et al., 2011, 2017). Accordingly, many neuronal precursor cells have been found in the graft suggesting that an important part of these transplanted cells may not be able to differentiate into dopaminergic neurons. A pertinent question is therefore whether α -syn pathology can be transferred from the tissue to such neuronal precursors that may further propagate the disease.

In the present study, we used human iPS cell-derived neuronal precursors (hNPCs) differentiated towards the dopaminergic lineage to investigate whether these cells could have an active role in the internalization and propagation of α -syn fibrils. We demonstrate that α -syn fibrils are internalized by hNPCs and are localized in

lysosomal vesicles where they are subjected to degradation. Further, we observed that α -syn fibrils can be transferred between hNPCs, primarily by cell-cell contact and to a much lesser extent through a secretory route. In particular, we showed that hNPCs are able to form TNT-like structures (Sartori-Rupp et al., 2019) and that α -syn fibrils can be found inside these structures formed between two different population of hNPCs.

Overall, our *in vitro* study reveals that hNPCs are capable of fibrillary α -syn uptake, intercellular transfer and degradation and may play a role in modulating α -syn pathology.

2.Materials and Methods

2.1 Culture of human iPSCs and differentiation to dopaminergic neuronal precursor cells (NPCs)

WT and A53T-iPSC lines were generated and characterized as previously described (Kouroupi et al., 2017). iPSCs were grown in pre-coating Geltrex (Life Technologies) plates in medium TeSR™-E8™ (StemCell Technologies). ReLeSR (StemCell Technologies) was used to passage iPSCs weekly. WT and A53T α -syn iPSCs were dissociated with EDTA 0,5mM for 2 min at 37°C and re-suspended in falcons with iPSC medium TeSR™-E8™ (StemCell Technologies). iPSC clumps were allowed to sink for ten minutes, were then resuspended in embryoid body (EBs) medium (1:1 DMEM/F12 and Neurobasal medium, 1x P/S, 1x N2, 2x B27 without vitamin A, 100 μ M β Mercaptoethanol) supplemented with 10 μ M Rock Inhibitor Y-27632 (Tebu), 10 μ M SB431542 (Tebu), 100nM LDN193189 (Tebu) and plated in Nunc no-treated flasks for suspension cell cultures (ThermoFisher Scientific). Medium was changed

every day until day 8 when EBs were plated onto p60 plates pre-coated with poly-L-ornithine 20µg/mL (Life Technologies) and laminin 10µg/mL (Sigma). The medium was then changed to NPC medium (Neurobasal A, 1x P/S, 1x N2, 2x B27 without vitamin A, 100 µM βMercaptoethanol, 1x Glutamax, supplemented with 200ng/ml SHH (R&d Systems), 100ng/ml FGF-8b (R&d Systems), 20ng/ml bFGF (Life Technologies), 20ng/ml EGF (Life Technologies) until day 12. At day 13 STEMdiff™ Neural Rosette Selection Reagent (StemCell Technologies) was used to select neural rosettes by micropipette. Rosettes were plated onto p60 plates pre-coated with poly-L-ornithine 20µg/mL (Life Technologies) and laminin 10µg/mL (Sigma) and were grown in NPC medium supplemented with only 20ng/ml bFGF (Life Technologies), passage p0. For next passages accutase (Sigma) was used. All experiments were performed using NPCs from p3 to p6 grown in NPC medium. All procedures for generating iPSC-NPCs were approved by Comité de Recherche Clinique, 825 Institut Pasteur, Paris (approval number 2015-034).

2.2 Expression, purification, preparation and labelling of alpha-syn fibrils

Human wild-type α-syn in pRK172, a construct containing α-syn that lacks cysteine because of mutagenesis of codon 136 (TAC to TAT) as described previously (Masuda et al., 2006), were transformed into *Escherichia coli* BL21 (DE3). Expression and purification were performed as described previously (Nonaka et al., 2005, 2010). The protein concentrations of monomeric α-syn were determined by RP-HPLC as described previously (Nonaka et al., 2005, 2010). Purified recombinant α-syn monomers (~5 mg/ml) containing 30 mM Tris-HCl, pH 7.5, 10 mM DTT, and 0.1% sodium azide were incubated at 37 °C with shaking using a horizontal shaker (TAITEC) at 200 rpm. After incubation for 7 days, the samples were ultracentrifuged

at 100,000 g for 20 min at room temperature, and the ppt fraction was recovered as α -syn fibrils. The samples were re-suspended in saline and ultracentrifuged again. The resultant pellets were re-suspended in saline and sonicated with an ultrasonic homogenizer (VP-5S, TAITEC). The fibrils were labelled with Alexa Fluor 568 Protein Labeling Kit (Invitrogen) according to the manufacturer's instructions. After incubation with Alexa Fluor dye, the samples were ultracentrifuged again. The pellets were re-suspended in 30 mM Tris-HCl, pH 7.5 and ultracentrifuged again. The labelled α -syn fibrils were re-suspended in saline containing 0.1% sodium azide. The protein concentration of the fibrils was determined by RP-HPLC as described previously (Nonaka et al., 2005, 2010). To check the *in vitro* seeding activity of the labelled fibrils, the fibrils (3 μ g) were added to 100 μ L of 1 mg/mL α -syn monomer in 30 μ M Thioflavin T and 80 mM Hepes, pH 7.5. Amyloid-like fibril formation was continuously monitored in terms of thioflavin T fluorescence (excitation 442 nm, emission 485 nm) with a plate reader (Varioskan Flash, Thermo Scientific).

2.3 Internalization assay of α -syn fibrils in hNPCs

hNPCs derived as described above were treated with 0.3 μ M of Alexa- 568 fluorescent-tagged human recombinant α -syn fibrils. Fibrils were diluted in the appropriate medium for each culture and sonicated for 5 min at 80% amplitude with a pulse cycle of 5s on and 2s off in an ultrasonic water bath Vibra-Cell 75041 (BioBlocks Scientific). Internalization was assessed at different time points after cells were washed using trypsin diluted 1:3 in PBS (3 times) to prevent the fibrils from remaining attached to the membrane, and finally culture medium was replaced (Fig. S2). All samples were fixed and then labeled with far red Wheat Germ Agglutinin (WGA) (Thermo Fisher) to visualize the plasma membrane.

175

176 **2.4 Co-culture systems of hNPCs**

177 In order to obtain two different cell populations, hNPCs donor cells were treated with
178 0.3 μ M of Alexa- 568 α -syn sonicated fibrils overnight. The following day, donor cells
179 were washed using trypsin diluted 1:3 in PBS (3 times) to remove eventual
180 fibrils that might have attached to the plasma membrane, detached by Accutase
181 (Sigma), counted and mixed (ratio 1: 1) in suspension with the acceptor cells (hNPCs
182 transfected by LV-GFP or labeled with CellMask Green (Invitrogen)), and co-cultured
183 for 24h. Then, cells were fixed and immunostained. For quantification of α -syn
184 transfer at least 100 cells were analysed in each independent experiment (n=3).

185

186 **2.5 Secretion experiment**

187 Donor cells were treated with 0.3 μ M of Alexa- 568 α -syn sonicated fibrils overnight.
188 The following day, the medium was removed and replaced with fresh for 24h. The
189 next day, the conditioned medium was added to acceptor cells (hNPCs transfected
190 by LV-GFP or labeled with CellMask Green (Invitrogen)) for 24h. After, cells were
191 fixed, stained and analysed. For quantification of α -syn transfer at least 100 cells
192 were analysed in each independent experiment (n=3).

193

194 **2.6 Cell viability assay by measuring LDH release**

195 Three independent experiments were performed following the manual instruction of
196 Cytotoxicity Detection Kit (LDH) (Roche). To measure the absorbance of the samples
197 96-well plate (Falcon) was read using Infinite® M200 PRO Tecan Fluorescence
198 Microplate Reader at 492nm.

199

2.7 Western Blot

hNPCs cultures were lysed using RIPA buffer (50mM Tris-HCl, pH 8.0, 150mM NaCl, 0.1% Triton X-100, 0.5% sodium deoxycholate, 0.1% sodium dodecyl sulphate (SDS), 1mM sodium orthovanadate, 1 mM NaF) containing protease inhibitor tablet (Roche), centrifuged for 15min at 3000 rpm. Protein concentration was estimated in the supernatant by Bradford assay (Biorad). Samples were subjected to 4-15% Mini Protean TGX Stain-Free gels (Biorad) and transferred onto 0.45µm pore size nitrocellulose membrane (Biorad). Non-specific binding sites were blocked in TBS 0.1% Tween 20/ 5% milk for 1 hour at RT followed by overnight incubation with mouse anti- α -synuclein (1:1000; BD Biosciences BD610787) or mouse anti- α Tubulin (1:2000; Sigma T9026) or rabbit anti-GAPDH (1:2000; Santa Cruz sc-25778). Incubation with appropriate HRP-conjugated secondary antibodies (GE Healthcare) was performed for 2 hours at RT and protein bands were visualized using Amersham ECL Prime Western Blotting Detection Reagent (GE Healthcare). The experiment was performed 3 times.

2.8 Immunocytochemistry of hNPCs

Immunostaining of hNPCs was performed following the same protocol. Cells were rinsed with PBS and fixed with 4% paraformaldehyde for 15min at 4°C, then cells were permeabilized and blocked with blocking solution (PBS 0.1% Triton, 5% FBS) for 1h in blocking solution. For only LAMTOR4 antibody cells were permeabilized 2 minutes with PBS 0.1% Triton and then blocked with PBS 10% BSA. Primary antibodies were incubated overnight at 4°C diluted in appropriate blocking solution. After rinsing with PBS, cells were incubated with Alexa-conjugated secondary antibody for 1h at room temperature (dilution 1:600), and nuclei were counterstained

with DAPI (1:1000; Sigma Aldrich). Coverslips were mounted using aqua-poly/mount (Polysciences). The antibodies used: rabbit anti-Nestin (1:200; Merck Millipore ABD69), mouse anti-PAX6 (1:50; Developmental Studies Hybridoma Bank), goat anti-Doublecortin (DCX, 1:100; Santa Cruz sc-8067), rabbit anti-Glial fibrillary acidic protein (GFAP, 1:500; DAKO Z0334), rabbit anti-LAMTOR4 (1 :1000 ; Cell Signaling 12284), mouse anti- α -synuclein Syn-1 (1:500; BD Biosciences BD610787), rabbit anti-LMX1 (1:1000 ; Merck Millipore AB10533), rabbit anti-SOX2 (1 :750 ; Abcam ab59776), rabbit anti-FoX2a (1:400 ; Abcam ab108422), chicken anti-MAP-2 (1:500; Merck Millipore AB15452), rabbit anti-TH (1 :500 ; Merck Millipore AB152).

For TNTs images cells were fixed with fixative solution 1 for 15 min (2%PFA, 0.05% glutaraldehyde and 0.2 M HEPES in PBS) and then with fixative solution 2 for another 15 min (4% PFA and 0.2 M HEPES in PBS).

2.9 LysoTracker Staining

To visualize lysosomes during co-culture and secretion experiment, donor and acceptor cells were labelled using LysoTracker Deep Red (Thermo Fisher Scientific L12492). Cells are incubated with the dye diluted 10nM in growth medium for 30 minutes at 37°C. After, the cells are rinsed 3 times with PBS and fixed with 4% PFA.

2.10 Genomic DNA analysis for detection of the p.A53T (G209A) mutation

Genomic DNA of iPSCs was extracted by Quick-DNA Microprep Kit (Zymo Research) following the manufacturer's recommended protocol. Specific primers were used for SNCA gene (Forward: GCTAATCAGCAATTTAAGGCTAG, Reverse: GATATGTTCTTAGATGCTCAG) and PCR products were digested by the restriction

enzyme Tsp45I (New England Biolabs). p.A53T (G209A) mutation results in a novel Tsp45I site and two additional fragments of 128 and 88 bp can be detected.

2.11 Acquisition and analysis of immunostained images at optical confocal microscopy

Images were acquired with an inverted laser scanning confocal microscope LSM700 (Zeiss), with a 63x objective (zoom 0.7 or 1). Images were acquired using the Zen acquisition software (Zeiss) and further processed with ICY software (Quantitative Image Analysis Unit, Institut Pasteur <http://icy.bioimageanalysis.org/>). In all experiments, it was acquired Z-stacks covering the whole volume of cells.

In details for the transfer experiments, in order to quantify the percentage of donor and acceptor cells containing α -syn puncta, the Z-stack was divided into the lower and upper part, segmenting only donor or acceptor cells, when possible, and then projecting the maximum intensity of those slices, using the ICY software. This was done in order to only have the whole donor or acceptor cell volume and to focus on what was inside the cells. Quantification of images was performed manually scrolling through the slices of the Z-stack to identify the puncta that were located inside the cell body based on nucleus identification and proximity. Overlapping cells were excluded from the analysis. Whereas all the images showed in the figures of hNPCs alone are projections of the entire Z- stack, the orthogonal views and images showed of co-culture experiments correspond to projections of selected slices of the Z-stack. For co-localization analysis all images were acquired using the same parameters at confocal microscope. At least 50 single cells from different images were analysed by JaCoP plugin in ImageJ. The Pearson correlation coefficient was used to quantify the

degree of colocalization between fluorophores α -syn fibrils puncta and lysosomes labelled by LAMTOR4 antibody.

Analysis was performed in 3 independent experiments.

2.12 Statistical analysis

Statistical analyses and graphs were performed using the GraphPad Prism version 6 software. All the results are expressed as the mean \pm s.e.m. For comparisons between two groups the Mann-Whitney test was used. Unless stated in the figure's legend, for comparisons between more than two groups, one-way ANOVA with Tukey's post hoc test was employed. In all cases, statistical significance was attributed when $p \leq 0.05$.

3. Results

3.1 Internalization of α -syn fibrils in hNPCs

To generate hNPCs, iPSCs produced from a healthy donor (Kouroupi et al., 2017) were differentiated to the dopaminergic lineage following a dual SMAD inhibition protocol (Chambers et al., 2009) as described in Materials and Methods section. For comparison, iPSCs generated from a patient carrying the G209A (p.A53T) mutation in the α -syn gene (Kouroupi et al., 2017) were also differentiated to hNPCs. After 25 days of differentiation, a committed population of neuronal precursor cells with dopaminergic (DA) identity was obtained. In particular, approximately 80% of cells were Sox2⁺/Nestin⁺ neuronal precursors, while co-staining with Nestin and Pax6 has shown that 51% of Nestin⁺ cells were Pax6⁺ committed neuronal precursors (39% in the total population) (Fig.S1A). GFAP⁺ cells comprised only 1.6% of the total cell population whilst the remaining cells (17.9% of the total population) were DCX⁺ early

born neurons. hNPCs were also assessed for expression of dopaminergic lineage markers showing that □31% were Lmx1⁺ and □25% Fox2a⁺ (Fig.S1A) . Finally, they were tested for their ability to differentiate *in vitro* into neurons, a fraction of which already expressed TH (□18% of cells positive) at 30 days (Fig.S1C).

We first examined whether recombinant Alexa 568 labeled human α-syn fibrils were capable of entering hNPCs. Time course experiments (Fig.1A, B) based on confocal images acquisition at different time points, revealed that α-syn fibrils were rapidly internalized with high efficiency. After 1h following α-syn fibril loading, the percentage of hNPCs containing fluorescent puncta was already around 80%, reaching 98% after 16h (Fig.1B). No differences between the two genotypes (WT and A53T-syn) were observed suggesting that the mutation does not impair internalization of α-syn fibrils. Then, we used a specific ICY software script to automatically detect and quantify the number and size of α-syn fibril puncta at different time points (Fig.1C). By this method, we found that both the average number and size of α-syn fibril puncta per cell did not significantly change from 3h to 16h, showing no significant difference between the two genotypes (Fig.1C).

These results indicate that hNPCs (WT and A53T-syn) are capable of uptaking α-syn fibrils very efficiently. We next analysed if the exposure to α-syn fibrils could generate a toxic effect in hNPCs.

3.2 Lactate dehydrogenase (LDH) release after exposure to α-syn fibrils in hNPCs

To investigate if α-syn fibrils could have toxic effects in hNPCs, we performed time course measurements of lactate dehydrogenase (LDH) release in the absence (control) and after exposure to α-syn fibrils (0.3 μM) (Fig.2). The results showed that

there was an increase in LDH release during the time of cell culture, as expected, but no significant increase was observed between control cells and cells (from both genotypes) exposed to α -syn fibrils. Thus, we concluded that α -syn fibrils were not toxic within the timeframe of our experiments (Fig.2) and the two genotypes did not show differences in terms of cell viability.

3.3 α -Syn fibrils are found in lysosomal vesicles in the cytosol of hNPCs

Previous studies showed that α -syn fibrils taken up from the medium are preferentially directed to the lysosomal compartment for degradation in different cell types (Hasegawa et al., 2011; Konno et al., 2012; Lee et al., 2005, 2008; Sung et al., 2001), thus next we analyzed the intracellular localization of α -syn fibrils following uptake by hNPCs. We found that also in hNPCs α -syn fibril puncta co-localize with lysosomal vesicles (Fig.3). We quantified the co-localization between fluorescent α -syn fibril puncta and lysosomes by using LAMTOR4 (a lysosomal marker) immunofluorescence (Pu et al., 2017). Taking into consideration the Pearson correlation coefficient (by JaCoP plugin, ImageJ, see material and methods), we found that after only 3h following α -syn fibril loading, α -syn fibrils were already inside lysosomes. Specifically, the percentages of co-localization during the experimental time frame (from 3h to 16h) were 52.8 ± 0.057 ; 58.5 ± 0.096 ; 62 ± 0.04 ; 45 ± 0.043 in WT hNPCs and 49 ± 0.04 ; 56 ± 0.03 ; 56 ± 0.043 ; 47 ± 0.02 in A53T hNPCs (Fig.3A). The fibrils persisted in lysosomes without significant differences in terms of their co-localization even after 16h. Moreover, the subcellular localization did not show any significant differences between the two genotypes. These results suggest that also in hNPCs, fibrils are directed to the lysosomal compartment and the A53T mutation does not affect this process.

348

349 **3.4 α -Syn fibrils are degraded rapidly in hNPCs**

350 We have previously shown that the ability of lysosomes to degrade up-taken α -syn
351 fibrils is cell type dependent (Loria et al., 2017). To address if α -syn fibrils stored in
352 lysosome compartments can be degraded by hNPCs, we quantified the total amount
353 of α -syn by Western Blot at different time points. hNPCs were loaded, or not (control
354 sample), with α -syn fibrils for 16h, then the cells were washed, kept in culture and
355 lysed at 16h, 1 day and 3 days. As previously reported (Bayer et al., 1999; Galvin et
356 al., 2001; Raghavan et al., 2004), endogenous α -syn was detected at low levels in
357 control hNPCs and increased considerably upon 16h exposure to α -syn fibrils.
358 Surprisingly, we observed that in both genotypes α -syn fibrils were degraded very
359 efficiently. In particular, significant degradation was observed between 1 day and 3
360 days (Fig.4A, B).

361 To confirm that this degradation was correlated to lysosome activity, we performed
362 the same experiment described above, adding for 36h two inhibitors of lysosomal
363 proteases: E64D (a membrane-permeable inhibitor of cathepsins B, H, and L) plus
364 pepstatin A (an inhibitor of cathepsins D and E)(Li et al., 2013; Yang et al., 2013) in
365 order to block degradation and visualize accumulation of fibrils inside the cells.
366 Indeed, after treatment with E64D (20 μ M) and pepstatin A (20 μ M) (E+P), we could
367 monitor by WB the accumulation of α -syn fibrils as compared with control (sample
368 without inhibitors lysed at the same time) (Fig. 4C). Qualitative immunofluorescence
369 experiments confirmed that the treatment with the two inhibitors induced the
370 accumulation of fibrils into hNPC; interestingly the pictures show that after 36H
371 treatment fibrils accumulate outside the lysosomes labeled by lysotracker (Fig. S2).

Overall this result demonstrated that hNPCs are able to degrade α -syn fibrils within 3 days following uptake and that this degradation occurs via the lysosomal pathway.

3.5 α -Syn fibrils can be transferred between hNPCs

In previous studies, we demonstrated that neuron-like CAD cells, primary murine cortical neurons and murine astrocytes propagate α -syn fibrils to other cells, and the transfer occurs preferentially inside lysosomal vesicles through tunneling nanotubes (TNTs) (Abounit et al., 2016; Loria et al., 2017). In order to assess if hNPCs could also have a role in the spreading of α -syn fibrils we tested their transfer ability in a co-culture system. hNPCs were first loaded overnight with Alexa 568 labelled- α -syn fibrils (donor cells). The following day donor cells were washed using trypsin diluted 1:3 in PBS (3 times) to remove eventual fibrils that might have attached to the plasma membrane (Fig. S3), and co-cultured for 24h at a 1:1 ratio with hNPCs expressing GFP by lentiviral transduction (LV-GFP) that allowed to distinguish acceptor cells that were labeled in green (Fig.5A). Transfer of α -syn fibrils was monitored by immunofluorescence and quantitative confocal microscopy. After 24h in co-culture, we observed that both donor and acceptor cells contained α -syn puncta (Fig.5B). By Z-stack imaging and orthogonal projection of cells we confirmed the presence of α -syn puncta within the acceptor cells (Fig.5B). Using ICY software we automatically detected and quantified the number of α -syn puncta. Under these experimental conditions, we found that the average number of α -syn puncta inside acceptor cells was 11.8 ± 1.31 in WT hNPCs and 15.34 ± 2.98 in A53T hNPCs (Fig.5C) without significant differences in α -syn fibril transfer between genotypes. Importantly, by using α -syn antibodies we could confirm that α -syn fibrils were actually transferred in acceptor cells as we observed co-localization between α -syn

antibodies and Alexa 568 puncta (Fig.S4). These data indicated that hNPC were able to efficiently transfer α -syn fibrils between them.

To understand whether this transfer occurred mainly through a cell to cell dependent mechanism next we measured the amount of transfer occurring through the secretory pathway. Specifically, we monitored whether α -syn fibrils could be secreted by hNPCs in the medium and subsequently taken up from acceptor cells. To this aim, hNPCs were first loaded overnight with Alexa 568 labelled- α -syn fibrils (donor cells), then the medium was removed and replaced for 24h. Next, the conditioned medium of 24 hours from the donor cells was added to acceptor cells (plated in different dishes) for 24h (Fig.5D). We observed that α -syn fibrils were secreted by hNPCs and uptaken by acceptor cells after 24h. However, the average number of puncta per acceptor cell was low compared with the co-culture system (2.7 ± 0.6 in WT hNPCs and 2.9 ± 0.5 in A53T hNPCs) (Fig.5E, F). Consistently, we also observed that the percentage of acceptor cells containing α -syn puncta was lower in acceptor cells exposed to conditioned medium compared with the co-culture conditions (33.60 ± 7.00 vs 65.53 ± 4.165 in WT hNPCs and 32.75 ± 4.45 vs 57.29 ± 2.714 in A53T hNPCs) (Fig.5 G). Altogether these data suggest that the amount of transfer through a secretory pathway was less efficient. Moreover, we could show that hNPCs are able to form numerous TNT-like-structures between themselves. These structures contained α -syn puncta, suggesting that α -syn fibrils could be transferred through these connections (Fig.5 H), similar to what was shown in neuronal cell lines (Abounit et al., 2016).

Finally, we investigated the subcellular localization of α -syn puncta in acceptor cells both after cell-to-cell mediated transfer and through secretion in the conditioned medium. To this aim we used lysotracker to detect lysosomal vesicles in acceptor

cells. In both conditions α -syn puncta were found inside lysosomes in acceptor cells similar to donor cells (Fig.S5); co-localization analysis between fibrils and lysotracker did not show any significant differences between the two conditions (57 ± 0.02 in co-culture and 59 ± 0.02 in secretion). This is consistent with previous data in neuronal cells, indicating that α -syn transfer by cell-to-cell contact occurs in lysosomes. Furthermore, this data indicates that in the case of transfer following secretion, after internalization α -syn is delivered to lysosomes also in acceptor cells. Overall these data indicate that hNPCs have the ability to degrade α -syn fibrils but could also spread them from one cell to another, embracing the respective characteristics of astrocytes and neurons (Abounit et al., 2016; Loria et al., 2017). Also in hNPCs, α -syn fibrils may spread more efficiently by cell-to-cell contact as previously demonstrated in neuronal cells and primary mouse neurons (Abounit et al., 2016; Loria et al., 2017). Moreover, the observation of TNT-like structures with α -syn puncta inside them, suggests that these connections could have a role in the propagation of α -syn also in neuronal precursors.

4.Discussion

Experimental studies in rodent and primate models as well as clinical trials (Yasuhara et al., 2017) have highlighted the potential of cell transplantation for treatment of Parkinson's disease in order to compensate for neuronal loss and improve disease symptoms (Freed et al., 2001; Wernig et al., 2008; Kriks et al., 2011; Doi et al., 2014; Kikuchi et al., 2017). Several cellular populations have been considered for engraftment, including human embryonic or induced pluripotent stem cell-derived neuronal precursors (Xiao et al., 2016; Kikuchi et al., 2017; Zhang et al., 2018). For a successful outcome, transplanted cells should display long-term survival, differentiate

efficiently into the appropriate neuronal phenotype and confer functional recovery. However, over the years several shortcomings have raised caution, nonetheless because a significant fraction of grafted cells remains in an undifferentiated precursor state (Freed et al., 2001; Kikuchi et al., 2011; Kriks et al., 2011; Kikuchi et al., 2017). An additional concern is the possibility that pathology may be transmitted from the host brain to the graft, resulting amongst others in the emergence of pathological protein species within the grafted cells (Hansen et al., 2011; Desplats et al., 2009; Kordower et al., 2011; Angot et al., 2012). Therefore, careful characterization of the properties of transplantable cells is of major importance.

Previous evidence indicates that grafted neurons can develop Lewy bodies, suggesting host-to-graft disease propagation (Desplats et al., 2009; Lee et al., 2008). Moreover, it is well recognized that α -syn aggregates can spread throughout the nervous system in a prion-like manner (Braak et al., 2003) and different studies *in vitro* reveal that α -syn fibrils can transfer from neuron-to-neuron (Domert et al., 2016; Freundt et al., 2012), neurons-to-astrocytes and between astrocytes (Loria et al., 2017). Taking into consideration this knowledge, we decided to study *in vitro*, whether human iPS cell-derived NPCs may have a role in the spreading or in the degradation of α -syn fibrils, as previously demonstrated for neurons and astrocytes (Loria et al., 2017).

Our *in vitro* data demonstrates that hNPCs are able to take up α -syn fibrils very efficiently, as previously shown for neurons and astrocytes. Moreover, like in neurons and astrocytes, these fibrils are directed to the lysosomal compartment as soon as 3h after internalization (Domert et al., 2016; Freeman et al., 2013; Mak et al., 2010; Sacino et al., 2017). However, in neurons α -syn fibrils that are initially directed to lysosomes, may escape and accumulate within the cell through an as yet unknown

472 mechanism (Freeman et al., 2013; Victoria and Zurzolo, 2017). On the other hand, in
473 astrocytes α -syn fibrils are efficiently degraded suggesting that astrocytes play an
474 important protective role in PD and possibly other brain pathologies characterized by
475 protein aggregates (Loria et al., 2017). Given the different behavior of neurons and
476 astrocytes in response to fibril internalization, it was interesting to investigate how
477 multipotential cells, like hNPCs that can give rise to both neurons and glia -
478 astrocytes as well as oligodendrocytes – *in vitro* as well as *in vivo* (Gunhanlar et al.,
479 2018; Lim and Alvarez-Buylla, 2016; Shi et al., 2012), would perform in the presence
480 of α -syn fibrils. Our *in vitro* experiments revealed that in hNPCs, α -syn fibrils not only
481 co-localize with lysosomes but they are quite efficiently cleared from the cell within 3
482 days. Surprisingly fibril degradation does not start immediately, but initiates one day
483 after fibril loading and continues over three days. Using two specific lysosomal
484 inhibitors (E64D plus pepstatin A) we could confirm that fibril degradation occurs
485 through the lysosome pathway in hNPCs. We did not observe any difference
486 between the two genotypes (WT or A53T-syn), suggesting that the mutation at this
487 early cell state does not affect the intracellular fate of fibrils inside the lysosome nor
488 the degradation pathway. Furthermore, our co-localization analysis shows that
489 around 40% of α -syn fibrils does not co-localize with lysosomal vesicles and is not
490 inside other organelles (data not shown) suggesting that they could remain free in the
491 cytoplasm. Interestingly, this data are very similar to those reported by Flavin et al.,
492 2017 where co-localization analysis in SH-SY5Y cells shows that 55% of α -syn fibrils
493 co-localizes with chGal3, Lysotracker or both markers, while the other half co-
494 localizes with neither marker (Flavin et al., 2017).

495 The ability of misfolded α -syn to aggregate and spread throughout the brain has
496 strong implications for PD progression. Here, we demonstrate using 24h co-culture

497 experiments that hNPCs can also transfer α -syn fibrils. In particular, we observe that
498 hNPCs can form TNT-like structures. Occasionally, we also observe α -syn puncta
499 inside these structures. This suggests that the transfer of α -syn between hNPCs
500 could be TNT-mediated as previously shown in rodent neurons and human
501 astrocytes (Abounit et al., 2016; Rostami et al., 2017). However, in the absence of a
502 specific marker for TNTs, we cannot provide quantitative data to correlate the
503 number puncta inside TNTs with cell-to-cell transfer. Indeed TNTs are very dynamic
504 and fragile structures so, although we have set up specific fixation conditions
505 (Abounit et al., 2015; Sartori-Rupp et al., 2019) many of them do not resist the
506 treatment. This represents a limitation of our study and hopefully will be overcome
507 with the improvement of the techniques and the discovery of specific markers.

508 Apart from a cell contact-dependent transfer, we demonstrated that α -syn fibrils could
509 also be secreted by hNPCs, in agreement with previous studies reporting that α -syn
510 secretion could occur and could be mediated at least in part, by exosomes or other
511 extracellular vesicles (Emmanouilidou et al., 2010; Alvarez-Erviti et al., 2011; Danzer
512 et al., 2012; Kunadt et al., 2015; Minakaki et al., 2018). However, in our conditions it
513 appears that the transfer mediated by secretion in the supernatant is much less
514 efficient compared with the transfer mediated by cell-to-cell contact, both in terms of
515 number of α -syn puncta transferred/cell and in terms of number of acceptor cells that
516 received α -syn. This is similar to what was previously found in mouse neuronal cells
517 and primary neurons (Abounit et al., 2016; Loria et al., 2017). Nonetheless our
518 experiments cannot rule out the possibility that local secretion could mediate part of
519 the transfer in cells that are in close apposition, in the absence of synapses. Thus
520 this hypothesis should be considered in future studies.

In summary, the present study provides evidence for the involvement of hNPCs in both the degradation and transfer of α -syn fibrils. This opens a new perspective to be considered in therapeutic strategies involving cell transplantation for treatment of PD and other synucleinopathies. Our work demonstrated the ability of hNPCs to clear up α -syn fibrils, suggesting that these cells could have a similar protective role as observed for astrocytes (Loria et al., 2017). On the other hand, hNPCs can also transfer α -syn fibrils between them and probably between hNPCs and other brain cells, raising the possibility that continuous exposure to α -syn fibrils could affect the lysosomal pathway and contribute to α -syn accumulation and spreading. Notwithstanding that such a possible α -syn accumulation in hNPCs could influence their differentiation into mature neurons. It still remains unexplored whether endogenous α -syn has a role in the transition from hNPCs to mature neurons. It appears that α -syn is almost entirely expressed in nerve terminals of the adult brain, but it has also been found in the perikarya during development (Bayer et al., 1999; Galvin et al., 2001; Raghavan et al., 2004). This may indicate that a change in the subcellular localization of α -syn, could have a function in determining neuronal differentiation and maturation, and particularly synapse formation. Future studies should address these issues.

Acknowledgments

We are thankful to Dr. Michael Henderson for the proofread of this manuscript; all lab members of CZ group for all suggestions and technical supports in this project.

This work was supported by the Programme Transversaux De Recherche - PTR (523) from Institut Pasteur (R.M. and C.Z), Agence Nationale de la Recherche [ANR-16-CE16-0019-01](C.Z), Fondation pour la Recherche Médicale [FRM-2016-

DEQ20160334896] (C.Z), France Alzheimer [AAP SM 2017#1674] (C.Z), LECMA-
VAINCRE ALZHEIMER [2016/FR-16020] (C.Z), Scientific Research on Innovative
Areas (Brain Protein Aging and Dementia Control) [JP26117005] from MEXT (M.H.),
Scientific Research on Brain Mapping by Integrated Neurotechnologies for Disease
Studies (Brain/MINDS) [JP14533254] from AMED (M.H.), JST CREST (JP18071300)
(M.H.), Brain Science Foundation (T.N.).

Declaration of interests

The authors declare no competing interests.

References

- Abounit, S., Delage, E., and Zurzolo, C. (2015). Identification and Characterization of Tunneling Nanotubes for Intercellular Trafficking. *Curr Protoc Cell Biol* 67, 12.10.1-21.
- Abounit, S., Bousset, L., Loria, F., Zhu, S., de Chaumont, F., Pieri, L., Olivo - Marin, J., Melki, R., and Zurzolo, C. (2016). Tunneling nanotubes spread fibrillar α -synuclein by intercellular trafficking of lysosomes. *EMBO J* 35, 2120–2138.
- Allen Reish, H.E., and Standaert, D.G. (2015). Role of α -synuclein in inducing innate and adaptive immunity in Parkinson disease. *J Parkinsons Dis* 5, 1–19.
- Alvarez-Erviti, L., Seow, Y., Schapira, A.H., Gardiner, C., Sargent, I.L., Wood, M.J.A., and Cooper, J.M. (2011). Lysosomal dysfunction increases exosome-mediated alpha-synuclein release and transmission. *Neurobiol. Dis.* 42, 360–367.
- Angot, E., Steiner, J.A., Lema Tomé, C.M., Ekström, P., Mattsson, B., Björklund, A., and Brundin, P. (2012). Alpha-synuclein cell-to-cell transfer and seeding in grafted dopaminergic neurons in vivo. *PLoS ONE* 7, e39465.
- Bayer, T.A., Jäkälä, P., Hartmann, T., Egensperger, R., Buslei, R., Falkai, P., and Beyreuther, K. (1999). Neural expression profile of alpha-synuclein in developing human cortex. *Neuroreport* 10, 2799–2803.
- Braak, H., Sandmann-Keil, D., Gai, W., and Braak, E. (1999). Extensive axonal Lewy neurites in Parkinson's disease: a novel pathological feature revealed by alpha-synuclein immunocytochemistry. *Neurosci. Lett.* 265, 67–69.

576 Braak, H., Del Tredici, K., Rüb, U., de Vos, R.A.I., Jansen Steur, E.N.H., and Braak, E. (2003).
577 Staging of brain pathology related to sporadic Parkinson's disease. *Neurobiol. Aging* 24,
578 197–211.

579 Brundin, P., and Melki, R. (2017). Prying into the Prion Hypothesis for Parkinson's
580 Disease. *J. Neurosci.* 37, 9808–9818.

581 Chambers, S.M., Fasano, C.A., Papapetrou, E.P., Tomishima, M., Sadelain, M., and Studer, L.
582 (2009). Highly efficient neural conversion of human ES and iPS cells by dual inhibition of
583 SMAD signaling. *Nat. Biotechnol.* 27, 275–280.

584 Conway, K.A., Harper, J.D., and Lansbury, P.T. (1998). Accelerated in vitro fibril
585 formation by a mutant alpha-synuclein linked to early-onset Parkinson disease. *Nat.*
586 *Med.* 4, 1318–1320.

587 Danzer, K.M., Kranich, L.R., Ruf, W.P., Cagsal-Getkin, O., Winslow, A.R., Zhu, L.,
588 Vanderburg, C.R., and McLean, P.J. (2012). Exosomal cell-to-cell transmission of alpha
589 synuclein oligomers. *Mol Neurodegener* 7, 42.

590 Desplats, P., Lee, H.-J., Bae, E.-J., Patrick, C., Rockenstein, E., Crews, L., Spencer, B., Masliah,
591 E., and Lee, S.-J. (2009). Inclusion formation and neuronal cell death through neuron-to-
592 neuron transmission of alpha-synuclein. *Proc. Natl. Acad. Sci. U.S.A.* 106, 13010–13015.

593 Doi, D., Samata, B., Katsukawa, M., Kikuchi, T., Morizane, A., Ono, Y., Sekiguchi, K.,
594 Nakagawa, M., Parmar, M., and Takahashi, J. (2014). Isolation of human induced
595 pluripotent stem cell-derived dopaminergic progenitors by cell sorting for successful
596 transplantation. *Stem Cell Reports* 2, 337–350.

597 Domert, J., Sackmann, C., Severinsson, E., Agholme, L., Bergström, J., Ingelsson, M., and
598 Hallbeck, M. (2016). Aggregated Alpha-Synuclein Transfer Efficiently between Cultured
599 Human Neuron-Like Cells and Localize to Lysosomes. *PLoS ONE* 11, e0168700.

600 Emmanouilidou, E., Melachroinou, K., Roumeliotis, T., Garbis, S.D., Ntzouni, M., Margaritis,
601 L.H., Stefanis, L., and Vekrellis, K. (2010). Cell-produced alpha-synuclein is secreted in a
602 calcium-dependent manner by exosomes and impacts neuronal survival. *J. Neurosci.* 30,
603 6838–6851.

604 Flavin, W.P., Bousset, L., Green, Z.C., Chu, Y., Skarpathiotis, S., Chaney, M.J., Kordower, J.H.,
605 Melki, R., and Campbell, E.M. (2017). Endocytic vesicle rupture is a conserved
606 mechanism of cellular invasion by amyloid proteins. *Acta Neuropathol.* 134, 629–653.

607 Freed, C.R., Greene, P.E., Breeze, R.E., Tsai, W.Y., DuMouchel, W., Kao, R., Dillon, S.,
608 Winfield, H., Culver, S., Trojanowski, J.Q., et al. (2001). Transplantation of embryonic
609 dopamine neurons for severe Parkinson's disease. *N. Engl. J. Med.* 344, 710–719.

610 Freeman, D., Cedillos, R., Choyke, S., Lukic, Z., McGuire, K., Marvin, S., Burrage, A.M.,
611 Sudholt, S., Rana, A., O'Connor, C., et al. (2013). Alpha-synuclein induces lysosomal
612 rupture and cathepsin dependent reactive oxygen species following endocytosis. *PLoS*
613 *ONE* 8, e62143.

614 Freundt, E.C., Maynard, N., Clancy, E.K., Roy, S., Bousset, L., Sourigues, Y., Covert, M.,
615 Melki, R., Kirkegaard, K., and Brahic, M. (2012). Neuron-to-neuron transmission of α -
616 synuclein fibrils through axonal transport. *Ann. Neurol.* 72, 517–524.

617 Galvin, J.E., Schuck, T.M., Lee, V.M., and Trojanowski, J.Q. (2001). Differential expression
618 and distribution of alpha-, beta-, and gamma-synuclein in the developing human
619 substantia nigra. *Exp. Neurol.* 168, 347–355.

620 Gunhanlar, N., Shpak, G., van der Kroeg, M., Gouty-Colomer, L.A., Munshi, S.T.,
621 Lendemeijer, B., Ghazvini, M., Dupont, C., Hoogendijk, W.J.G., Gribnau, J., et al. (2018). A
622 simplified protocol for differentiation of electrophysiologically mature neuronal
623 networks from human induced pluripotent stem cells. *Mol. Psychiatry* 23, 1336–1344.

624 Hansen, C., Angot, E., Bergström, A.-L., Steiner, J.A., Pieri, L., Paul, G., Outeiro, T.F., Melki,
625 R., Kallunki, P., Fog, K., et al. (2011). α -Synuclein propagates from mouse brain to grafted
626 dopaminergic neurons and seeds aggregation in cultured human cells. *J. Clin. Invest.* 121,
627 715–725.

628 Hasegawa, T., Konno, M., Baba, T., Sugeno, N., Kikuchi, A., Kobayashi, M., Miura, E.,
629 Tanaka, N., Tamai, K., Furukawa, K., et al. (2011). The AAA-ATPase VPS4 regulates
630 extracellular secretion and lysosomal targeting of α -synuclein. *PLoS ONE* 6, e29460.

631 Karpinar, D.P., Baliya, M.B.G., Kügler, S., Opazo, F., Rezaei-Ghaleh, N., Wender, N., Kim, H.-
632 Y., Taschenberger, G., Falkenburger, B.H., Heise, H., et al. (2009). Pre-fibrillar alpha-
633 synuclein variants with impaired beta-structure increase neurotoxicity in Parkinson's
634 disease models. *EMBO J.* 28, 3256–3268.

635 Kikuchi, T., Morizane, A., Doi, D., Onoe, H., Hayashi, T., Kawasaki, T., Saiki, H., Miyamoto,
636 S., and Takahashi, J. (2011). Survival of human induced pluripotent stem cell-derived
637 midbrain dopaminergic neurons in the brain of a primate model of Parkinson's disease. *J*
638 *Parkinsons Dis* 1, 395–412.

639 Kikuchi, T., Morizane, A., Doi, D., Magotani, H., Onoe, H., Hayashi, T., Mizuma, H., Takara,
640 S., Takahashi, R., Inoue, H., et al. (2017). Human iPS cell-derived dopaminergic neurons
641 function in a primate Parkinson's disease model. *Nature* 548, 592–596.

642 Konno, M., Hasegawa, T., Baba, T., Miura, E., Sugeno, N., Kikuchi, A., Fiesel, F.C., Sasaki, T.,
643 Aoki, M., Itoyama, Y., et al. (2012). Suppression of dynamin GTPase decreases α -
644 synuclein uptake by neuronal and oligodendroglial cells: a potent therapeutic target for
645 synucleinopathy. *Mol Neurodegener* 7, 38.

646 Kordower, J.H., Dodiya, H.B., Kordower, A.M., Terpstra, B., Paumier, K., Madhavan, L.,
647 Sortwell, C., Steece-Collier, K., and Collier, T.J. (2011). Transfer of host-derived α
648 synuclein to grafted dopaminergic neurons in rat. *Neurobiol. Dis.* 43, 552–557.

649 Kouroupi, G., Taoufik, E., Vlachos, I.S., Tsioras, K., Antoniou, N., Papastefanaki, F., Chroni-
650 Tzartou, D., Wrasidlo, W., Bohl, D., Stellas, D., et al. (2017). Defective synaptic
651 connectivity and axonal neuropathology in a human iPSC-based model of familial
652 Parkinson's disease. *Proc. Natl. Acad. Sci. U.S.A.* 114, E3679–E3688.

653 Kriks, S., Shim, J.-W., Piao, J., Ganat, Y.M., Wakeman, D.R., Xie, Z., Carrillo-Reid, L.,
654 Auyeung, G., Antonacci, C., Buch, A., et al. (2011). Dopamine neurons derived from
655 human ES cells efficiently engraft in animal models of Parkinson's disease. *Nature* **480**,
656 547–551.

657 Kunadt, M., Eckermann, K., Stuendl, A., Gong, J., Russo, B., Strauss, K., Rai, S., Kügler, S.,
658 Falomir Lockhart, L., Schwalbe, M., et al. (2015). Extracellular vesicle sorting of α -
659 Synuclein is regulated by sumoylation. *Acta Neuropathol.* **129**, 695–713.

660 Lee, H.-J., Patel, S., and Lee, S.-J. (2005). Intravesicular localization and exocytosis of
661 alpha-synuclein and its aggregates. *J. Neurosci.* **25**, 6016–6024.

662 Lee, H.-J., Suk, J.-E., Bae, E.-J., Lee, J.-H., Paik, S.R., and Lee, S.-J. (2008). Assembly-
663 dependent endocytosis and clearance of extracellular alpha-synuclein. *Int. J. Biochem.*
664 *Cell Biol.* **40**, 1835–1849.

665 Li, M., Khambu, B., Zhang, H., Kang, J.-H., Chen, X., Chen, D., Vollmer, L., Liu, P.-Q., Vogt, A.,
666 and Yin, X.-M. (2013). Suppression of lysosome function induces autophagy via a
667 feedback down-regulation of MTOR complex 1 (MTORC1) activity. *J. Biol. Chem.* **288**,
668 35769–35780.

669 Lim, D.A., and Alvarez-Buylla, A. (2016). The Adult Ventricular-Subventricular Zone (V-
670 SVZ) and Olfactory Bulb (OB) Neurogenesis. *Cold Spring Harb Perspect Biol* **8**.

671 Loria, F., Vargas, J.Y., Bousset, L., Syan, S., Salles, A., Melki, R., and Zurzolo, C. (2017). α -
672 Synuclein transfer between neurons and astrocytes indicates that astrocytes play a role
673 in degradation rather than in spreading. *Acta Neuropathol.* **134**, 789–808.

674 Mak, S.K., McCormack, A.L., Manning-Bog, A.B., Cuervo, A.M., and Di Monte, D.A. (2010).
675 Lysosomal degradation of alpha-synuclein in vivo. *J. Biol. Chem.* **285**, 13621–13629.

676 Masuda, M., Dohmae, N., Nonaka, T., Oikawa, T., Hisanaga, S., Goedert, M., and Hasegawa,
677 M. (2006). Cysteine misincorporation in bacterially expressed human alpha-synuclein.
678 *FEBS Lett.* **580**, 1775–1779.

679 Minakaki, G., Menges, S., Kittel, A., Emmanouilidou, E., Schaeffner, I., Barkovits, K.,
680 Bergmann, A., Rockenstein, E., Adame, A., Marxreiter, F., et al. (2018). Autophagy
681 inhibition promotes SNCA/alpha-synuclein release and transfer via extracellular
682 vesicles with a hybrid autophagosome-exosome-like phenotype. *Autophagy* **14**, 98–119.

683 Nonaka, T., Iwatsubo, T., and Hasegawa, M. (2005). Ubiquitination of alpha-synuclein.
684 *Biochemistry* **44**, 361–368.

685 Nonaka, T., Watanabe, S.T., Iwatsubo, T., and Hasegawa, M. (2010). Seeded aggregation
686 and toxicity of {alpha}-synuclein and tau: cellular models of neurodegenerative diseases.
687 *J. Biol. Chem.* **285**, 34885–34898.

688 Nuber, S., Rajsombath, M., Minakaki, G., Winkler, J., Müller, C.P., Ericsson, M., Caldarone,
689 B., Dettmer, U., and Selkoe, D.J. (2018). Abrogating Native α -Synuclein Tetramers in Mice
690 Causes a L-DOPA-Responsive Motor Syndrome Closely Resembling Parkinson's Disease.
691 *Neuron* **100**, 75-90.e5.

692 Peelaerts, W., Bousset, L., Van der Perren, A., Moskalyuk, A., Pulizzi, R., Giugliano, M., Van
693 den Haute, C., Melki, R., and Baekelandt, V. (2015). α -Synuclein strains cause distinct
694 synucleinopathies after local and systemic administration. *Nature* 522, 340–344.

695 Pu, J., Keren-Kaplan, T., and Bonifacino, J.S. (2017). A Ragulator-BORC interaction
696 controls lysosome positioning in response to amino acid availability. *J. Cell Biol.* 216,
697 4183–4197.

698 Raghavan, R., Kruijff, L. de, Sterrenburg, M.D., Rogers, B.B., Hladik, C.L., and White, C.L.
699 (2004). Alpha-synuclein expression in the developing human brain. *Pediatr. Dev. Pathol.*
700 7, 506–516.

701 Rostami, J., Holmqvist, S., Lindström, V., Sigvardson, J., Westermarck, G.T., Ingelsson, M.,
702 Bergström, J., Roybon, L., and Erlandsson, A. (2017). Human Astrocytes Transfer
703 Aggregated Alpha-Synuclein via Tunneling Nanotubes. *J. Neurosci.* 37, 11835–11853.

704 Sacino, A.N., Brooks, M., Thomas, M.A., McKinney, A.B., Lee, S., Regenhardt, R.W.,
705 McGarvey, N.H., Ayers, J.I., Notterpek, L., Borchelt, D.R., et al. (2014). Intramuscular
706 injection of α -synuclein induces CNS α -synuclein pathology and a rapid-onset motor
707 phenotype in transgenic mice. *Proc. Natl. Acad. Sci. U.S.A.* 111, 10732–10737.

708 Sacino, A.N., Brooks, M.M., Chakrabarty, P., Saha, K., Khoshbouei, H., Golde, T.E., and
709 Giasson, B.I. (2017). Proteolysis of α -synuclein fibrils in the lysosomal pathway limits
710 induction of inclusion pathology. *J. Neurochem.* 140, 662–678.

711 Sartori-Rupp, A., Cordero Cervantes, D., Pepe, A., Gousset, K., Delage, E., Corroyer-
712 Dulmont, S., Schmitt, C., Krijnse-Locker, J., and Zurzolo, C. (2019). Correlative cryo-
713 electron microscopy reveals the structure of TNTs in neuronal cells. *Nat Commun* 10,
714 342.

715 Shi, Y., Kirwan, P., and Livesey, F.J. (2012). Directed differentiation of human pluripotent
716 stem cells to cerebral cortex neurons and neural networks. *Nat Protoc* 7, 1836–1846.

717 Sung, J.Y., Kim, J., Paik, S.R., Park, J.H., Ahn, Y.S., and Chung, K.C. (2001). Induction of
718 neuronal cell death by Rab5A-dependent endocytosis of alpha-synuclein. *J. Biol. Chem.*
719 276, 27441–27448.

720 Tan, E.-K., Chandran, V.R., Fook-Chong, S., Shen, H., Yew, K., Teoh, M.-L., Yuen, Y., and
721 Zhao, Y. (2005). Alpha-synuclein mRNA expression in sporadic Parkinson's disease. *Mov.*
722 *Disord.* 20, 620–623.

723 Victoria, G.S., and Zurzolo, C. (2017). The spread of prion-like proteins by lysosomes and
724 tunneling nanotubes: Implications for neurodegenerative diseases. *J Cell Biol* 216, 2633–
725 2644.

726 Wernig, M., Zhao, J.-P., Pruszak, J., Hedlund, E., Fu, D., Soldner, F., Broccoli, V.,
727 Constantine-Paton, M., Isacson, O., and Jaenisch, R. (2008). Neurons derived from
728 reprogrammed fibroblasts functionally integrate into the fetal brain and improve
729 symptoms of rats with Parkinson's disease. *Proc. Natl. Acad. Sci. U.S.A.* 105, 5856–5861.

Xiao, B., Ng, H.H., Takahashi, R., and Tan, E.-K. (2016). Induced pluripotent stem cells in Parkinson's disease: scientific and clinical challenges. *J Neurol Neurosurg Psychiatry* 87, 697–702.

Yang, Y., Hu, L., Zheng, H., Mao, C., Hu, W., Xiong, K., Wang, F., and Liu, C. (2013). Application and interpretation of current autophagy inhibitors and activators. *Acta Pharmacol. Sin.* 34, 625–635.

Yasuhara, T., Kameda, M., Sasaki, T., Tajiri, N., and Date, I. (2017). Cell Therapy for Parkinson's Disease. *Cell Transplant* 26, 1551–1559.

Zhang, Y., Ge, M., Hao, Q., and Dong, B. (2018). Induced pluripotent stem cells in rat models of Parkinson's disease: A systematic review and meta-analysis. *Biomed Rep* 8, 289–296.

Figure legends

Fig. 1 Time course of α -syn fibrils internalization in hNPCs.

A Immunostained for fluorescent Alexa 568- α -syn fibrils (red) and *Wheat germ agglutinin* (WGA) (gray) in WT (upper) and A53T (bottom) hNPCs at different time points. Scale bar 10 μ m.

B. Quantification of the number of Alexa 568-positive cells during the time. Data are shown as mean \pm s.e.m from three independent experiments. Detection was determined by confocal microscopy and ICY software.

C Quantification of the average number and size per cells of α -syn fibrils puncta in hNPCs (WT left bar graph, A53T right bar graph) at different time points. Detection was determined by confocal microscopy and ICY software. Ns, not significant by one-way Anova, Tukey's multiple comparison test. Data are shown as mean \pm s.e.m from three independent experiments.

Fig. 2 Cytotoxicity assay in hNPCs.

Cell toxicity was measured by LDH release in WT (left bar graph) and A53T (right bar graph) hNPCs. The bar graph represents the percentage of cytotoxicity in control and α -syn fibrils (0.3 μ M) condition at 16h, 1 day and 3 days. There were no significant differences between control (black bar) and α -syn -loaded (gray bar) cells at any of the time points evaluated. Ns, not significant by one-way Anova, Tukey's multiple comparison test. Data are shown as mean \pm s.e.m from three independent experiments.

Fig.3 α -syn fibrils are found in lysosomal vesicles in the cytosol of hNPCs at 3, 6, 12 and 16h following fibril loading.

A Percentage of co-localization between LAMTOR4 (marker for lysosome) and Alexa 568 α -syn fibrils considering Pearson correlation coefficient at different time points (WT left bar graph, A53T right bar graph). Data are shown as mean \pm s.e.m from three independent experiments.

B Representative confocal images of co-localization in WT (upper panel) and in A53T hNPCs (bottom panel). LAMTOR4 green, α -syn fibrils red, WGA gray. Intracellular localization of α -syn puncta in hNPCs was confirmed with the magnified orthogonal cross-section view (x/y , x/z , and y/z axes) that corresponds to a single slice of the Z-stack. Scale bars represent 10 μ m.

Fig.4 α -Syn fibrils degradation in hNPCs.

A Representative confocal images showing the degradation of fibrils at 16h, 1 day and 3 days in WT (upper panel) and A53T hNPCs (bottom panel); α -syn fibrils red, WGA gray. Scale bar 10 μ m.

B Representative immunoblot of α -syn fibril over time in WT and A53T hNPCs. Cell lysates (10 μ g) from control and α -syn fibril-loaded hNPCs overnight were collected at different time points (16h, 1 day and 3 days) and immunoblotted against α -syn (Syn-1) and α -tubulin (as a loading control). Bar graphs show the total amount α -syn fibrils over time in WT (left panel) and A53T (right panel) hNPCs. Data represent the mean \pm sem of at least three independent experiments (One-way Anova, Tukey's multiple comparison test, * $p < 0.05$, ** $p < 0.01$)

C Representative immunoblot of α -syn fibril without (control) or in the presence of E64D (20 μ M) plus pepstatin A (20 μ M) (E+P) for 36h in WT and A53T hNPCs. Immunoblotted against α -syn (Syn-1) and GAPDH (as a loading control). Data represent the mean \pm sem of two independent experiments (One-way Anova, Tukey's multiple comparison test, * $p < 0.05$, ns = not significant).

Fig.5 α -syn fibrils transfer efficiently between hNPCs after 24h in co-culture experiments.

A Schematic of the co-culture system design between WT or A53T hNPC (donor cells) and LV-GFP WT hNPC (acceptor cells).

B Representative Z-stack projection of confocal images of 24h co-cultured hNPCs. Intracellular localization of α -syn puncta in hNPCS was confirmed with the magnified orthogonal cross-section view (x/y , x/z , and y/z axes) that corresponds to a single slice of the Z-stack. Scale bars represent 10 μ m. D= donor cells, A= acceptor cells. The yellow arrows show some examples of α -syn puncta inside acceptor cells.

C Bar graph showing the number α -syn puncta per acceptor hNPCs after 24 h in co-culture experiment. Ns, not significant by Mann Whitney test. Data show mean \pm sem of three independent experiments.

D Schematic of the secretion experiment design between WT or A53T hNPC (donor cells) and LV-GFP WT hNPC (acceptor cells).

E Representative Z-stack projection of confocal images of acceptor hNPCs after 24h of conditioned medium. The yellow arrows show some examples of α -syn puncta.

F Bar graph showing the number α -syn puncta per acceptor hNPCs after 24 h secretion experiment. Ns, not significant by Mann Whitney test. Data show mean \pm sem of three independent experiments.

G Bar graph showing the percentage of acceptor cells positive for α -syn puncta in co-culture and secretion system for both genotypes. Ns, not significant, *** $p < 0.001$ by Mann Whitney test. Data show mean \pm sem of three independent experiments.

H Representative confocal images showing TNT-like structures (yellow arrows) between hNPCs and in particular α -syn puncta inside of TNTs (magnification).

Fig.S1 Characterization of hNPCs.

A Immunostaining for Nestin, SOX2, Pax6 (markers of neural progenitor cells), DCX (marker of early born neurons), Lmx1a and FOX2a (markers of dopaminergic lineage specification). Scale bar 40 and 10 μ m.

B Detection of SNCA gene by PCR and the mutation A53T/G209A from human iPCS cell-derived dopaminergic NPCs.

C Neuronal differentiation of hNPCs at 30 days. Immunostaining for TH (Tyrosine hydroxylase) and MAP2 (dendritic marker). Nuclei are visualized with DAPI. Scale bar 10 μ m.

Fig.S2 Immunofluorescence of samples without (control) or with the treatment with lysosomal inhibitors E64D plus pepstatin A (E+P).

Lysotracker Deep Red staining and Alexa- 568 α -syn fibril after internalization (16H), and after 36 hours in control and in the presence of the inhibitors (E+P).

Scale bars represent 10 μ m.

Fig. S3 Internalization control of α -syn puncta in hNPCs.

Representative Z-stack projection of confocal images of hNPCs treated with 0.3 μ M of Alexa- 568 α -syn sonicated fibrils overnight, washed with trypsin (trypsin diluted 1:3 PBS) and re-plated. Intracellular localization of α -syn puncta in hNPCS was confirmed with the magnified orthogonal cross-section view (x/y , x/z , and y/z axes) that corresponds to a single slice of the Z-stack shows clearly the absence of fibrils still attached on the plasma membrane. Scale bars represent 10 μ m.

Fig. S4 Alexa 568 α -syn fibrils confirmed using α -syn Ab in co-culture condition.

Representative Z-stack projection of confocal images. The arrows show some examples of co-localization between Alexa 568 α -syn fibrils (red), α -syn revealed by Ab (far red) in acceptor cells after 24h of co-culture. Scale bar 10 μ m.

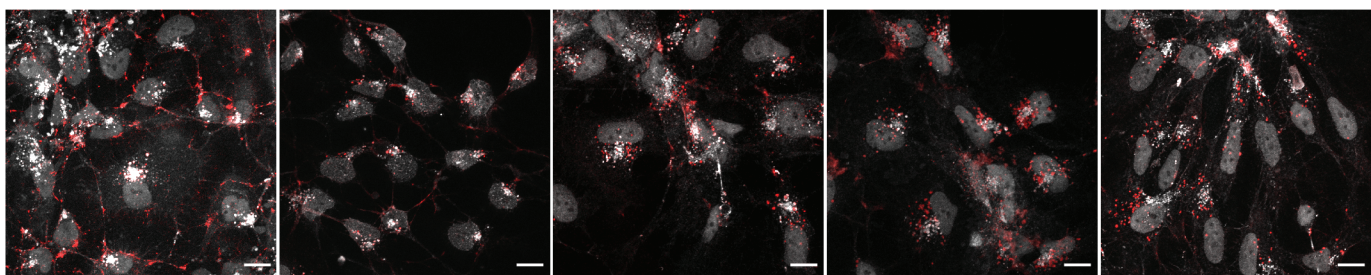
Fig.S5 Localization of Alexa 568 α -syn fibrils into lysosomes in acceptor cells in co-culture and secretion condition.

Representative Z-stack projection of confocal images. Immunostaining for lysosomes using Lysotracker Deep Red in acceptor cells and donor cells in co-culture (upper panel) and secretion (bottom panel) condition. The arrows show some examples of co-localization between fibrils and lysosomes. Scale bar 10 μ m. Percentage of co-

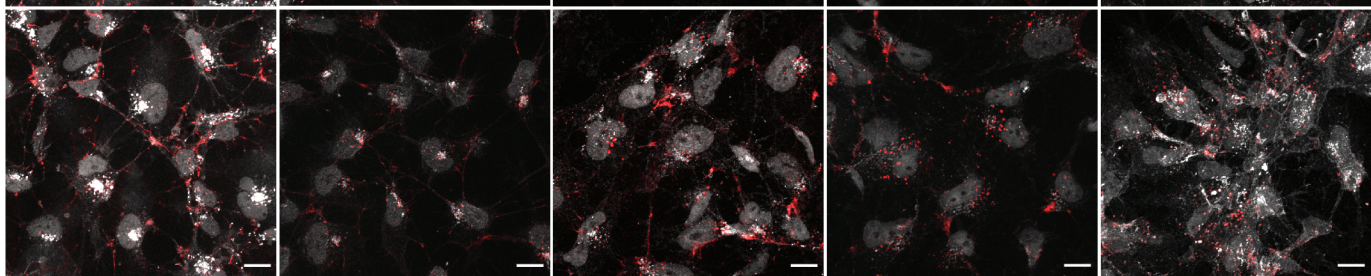
856 localization between LysoTracker Deep Red and Alexa 568 α -syn fibrils into acceptor
857 cells considering Pearson correlation coefficient.
858

WGA / Fibrils

WT



A53T



1H

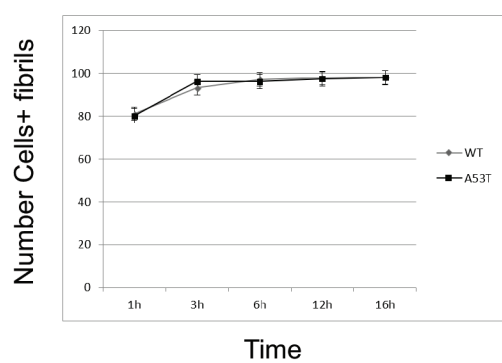
3H

6H

12H

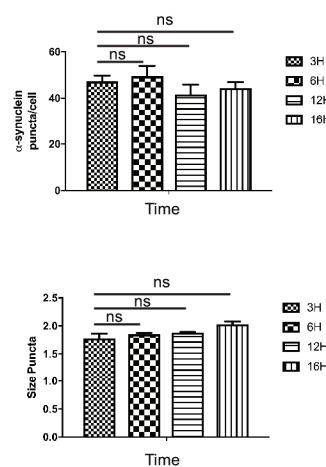
16H

B



C

WT



A53T

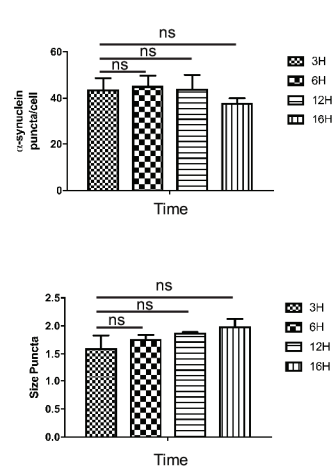


Figure 1

A

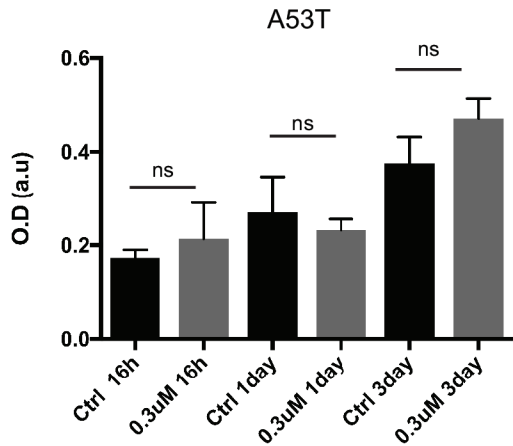
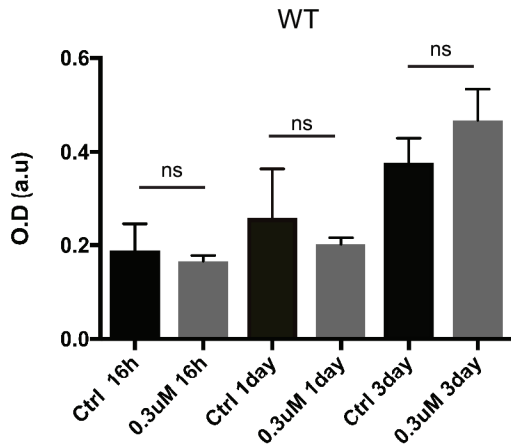
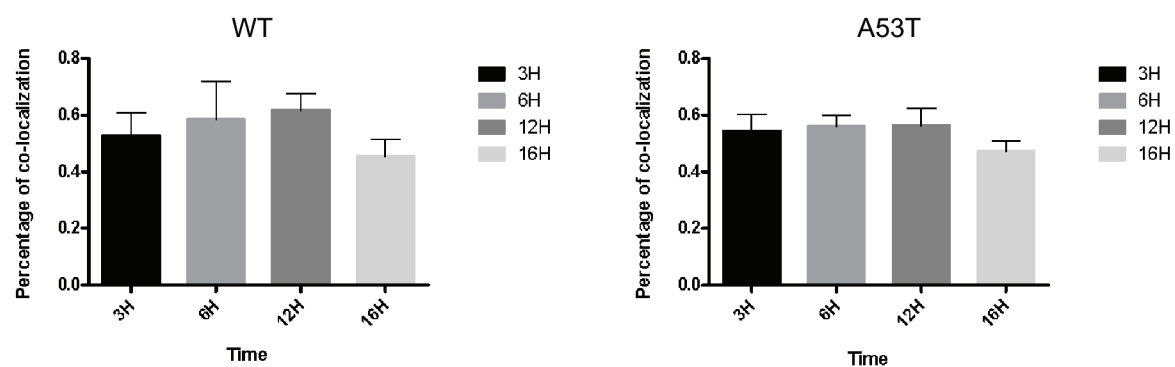


Figure 2

A



B

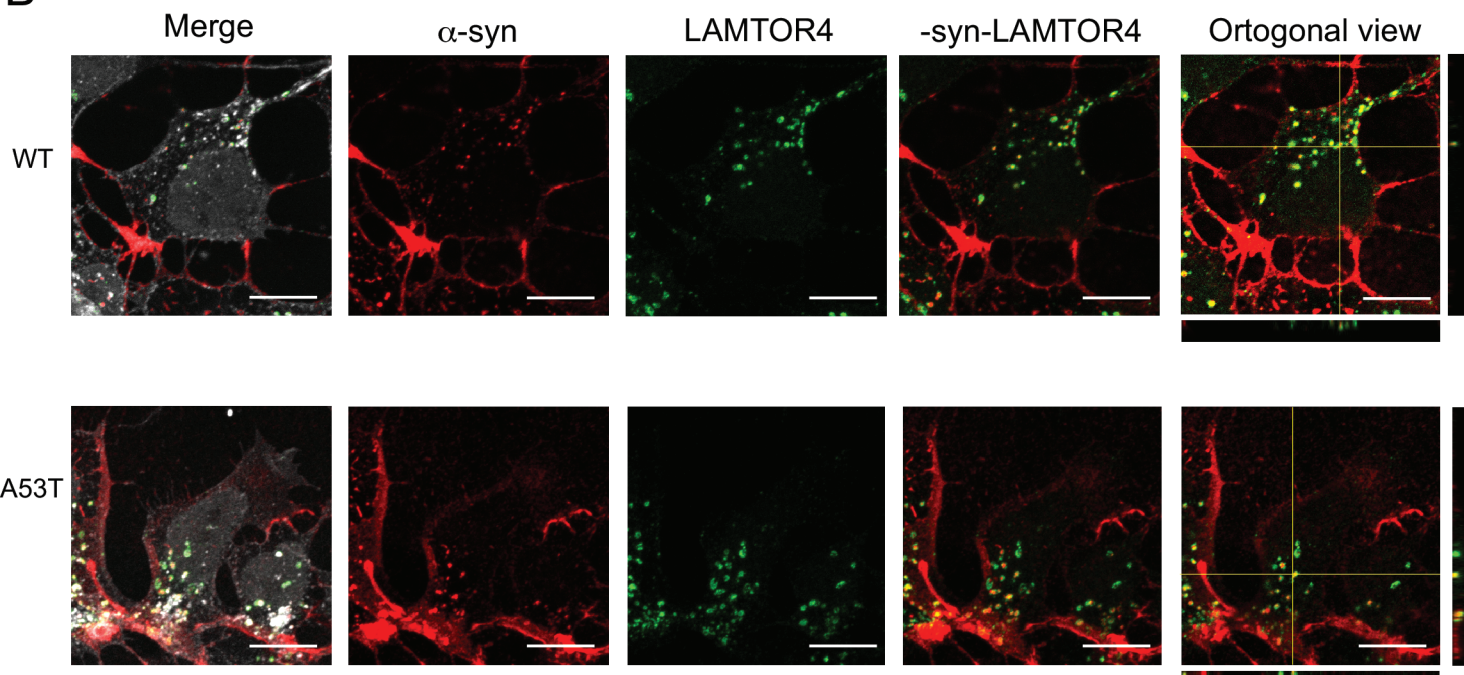
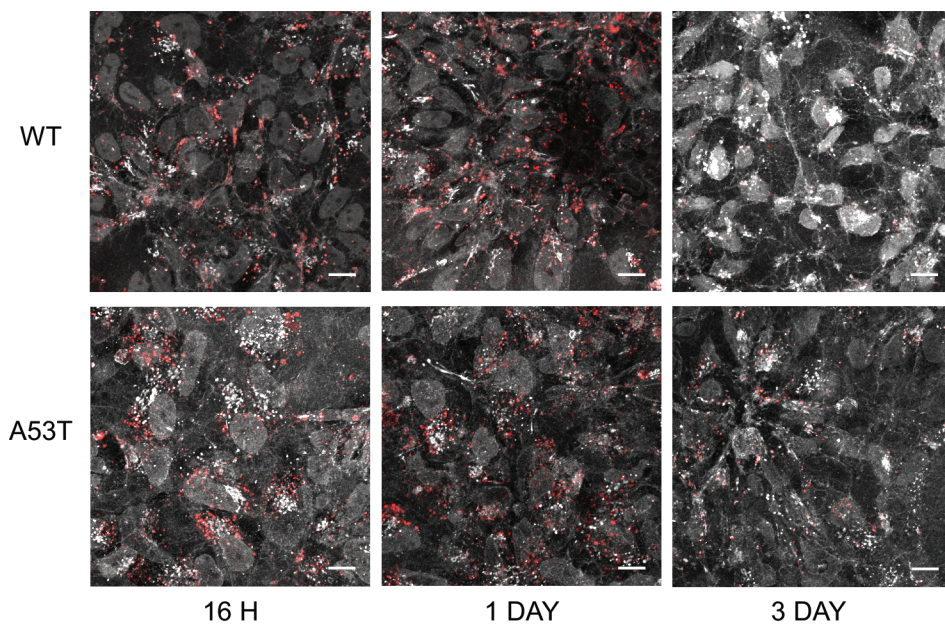


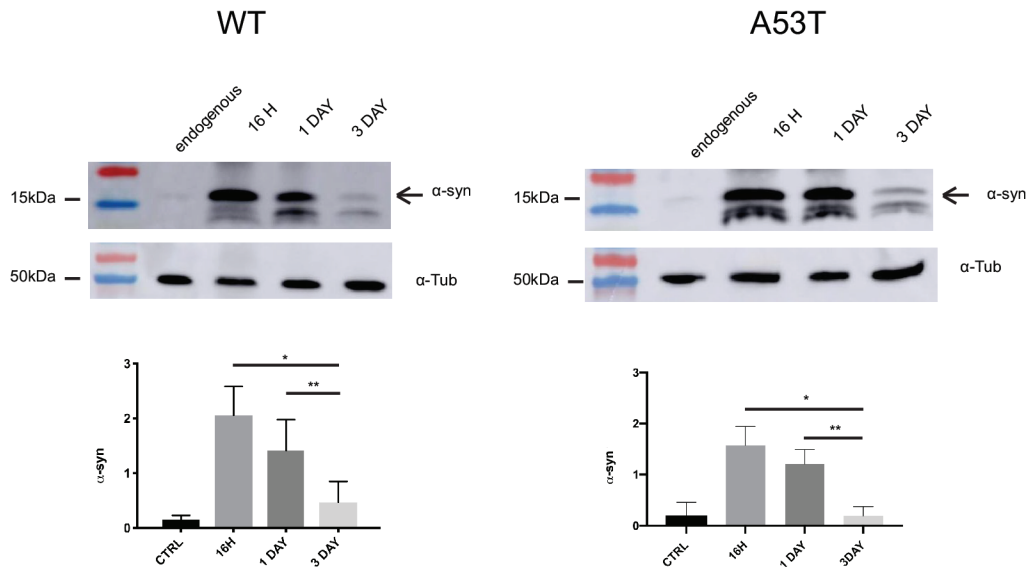
Figure 3

A

Fibrils / WGA



B



C

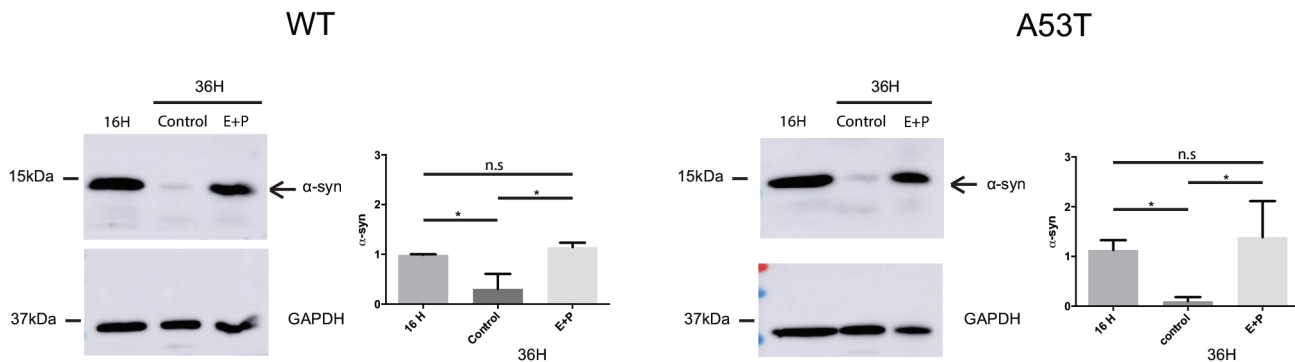


Figure 4

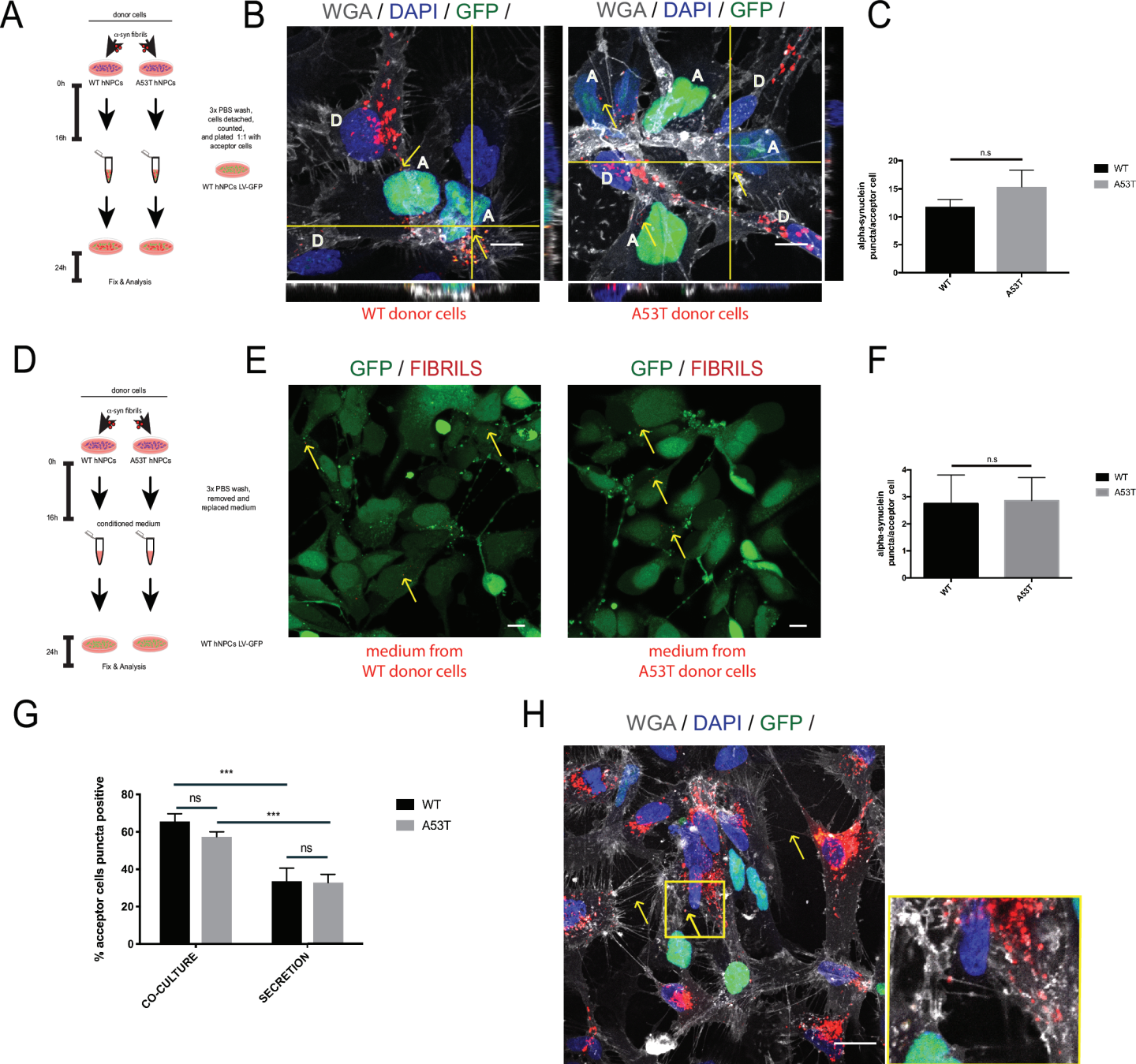


Figure 5